shRNA targeting α-synuclein prevents neurodegeneration in a Parkinson's disease model

Alevtina D. Zharikov, Jason R. Cannon, Victor Tapias, Qing Bai, Max P. Horowitz, Vipul Shah, Amina El Ayadi, Teresa G. Hastings, J. Timothy Greenamyre, and Edward A. Burton

Supplemental Figures 1 – 11

Supplemental Figure 1: Generation of a stable cell line expressing rat α-synuclein

We did not identify a cell line that expressed endogenous rat α-synuclein at sufficiently high levels to measure expression levels easily to evaluate siRNAs targeting of the *Snca* transcript. Consequently, we generated a stable sub-clone of immortalized Chinese hamster ovary (CHO) cells expressing rat α-synuclein for screening siRNAs. The transgene construct also expressed GFP from a bi-cistronic transcript, facilitating establishment of clonal lines by FACS sorting and enabling rapid screening of the activity of siRNAs targeting *Snca* by their effect on GFP expression.

A: The open reading frame of rat *Snca* was amplified using primers 5'-ATATGAATTCAGATGGATGTGTTCATGAAAG-3' and 5'-ATATGGATCCTCGTTAGGCTTCAGGCTCATA-3', and cloned into the BamHI/EcoRI sites of pIRES-EGFP2 (Clontech) to generate the expression cassette shown.

B: CHO cells were transfected with the resulting plasmid, selected for stable integration of the construct in medium containing G418, and subjected to fluorescent cell sorting to isolate clones expressing GFP at high levels. A single clonal cell line was established, which showed bright GFP fluorescence by microscopy and robust α-synuclein expression by western blot. The α-synuclein immunoreactive band could be readily quantified relative to β-actin using near-infrared (nIR) fluorophore-conjugated secondary antibodies and a LICOR infrared scanning system. The panel shows a western blot containing 10µg or 20µg of protein lysate from native CHO cells compared with CHO-synuclein cells. The blot was probed simultaneously using primary antibodies to α-synuclein and β-actin, which were imaged using two different nIR channels. The signal from this assay has a wide linear range allowing quantitative determination of protein abundance relative to the loading control.

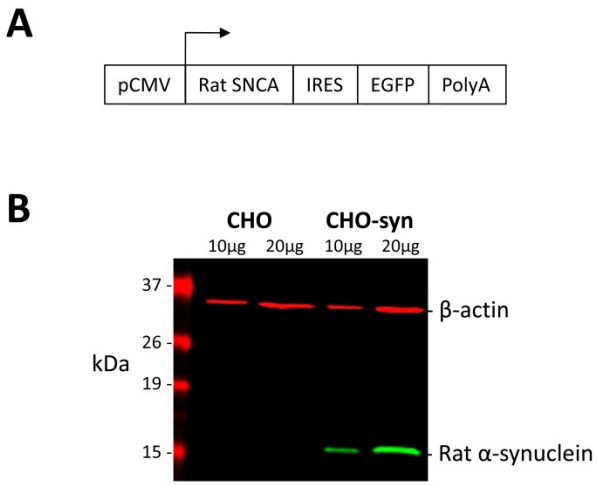

Supplemental Figure 2: Selection of siRNAs targeting rat SNCA

A,B: The *Snca* transcript encoding α-synuclein was analyzed for potential siRNA target sites using an online tool (https://rnaidesigner.lifetechnologies.com/rnaiexpress/design.do). The identified sites were compared with the sequences of *Sncb* and *Sncg*, encoding β-synuclein and γ-synuclein respectively, and sites showing significant homology between the transcripts were rejected. We also rejected target sites showing significant homology to other genes, using BLAST search. This left three potential siRNA target sites within the open reading frame, numbered relative to the first base in the *Snca* transcript. In panel B, the sequences of these three siRNAs are shown underlined in bold, with mismatch bases in the *Sncb* and *Sncg* transcripts labeled in green.

C: Double strand siRNAs corresponding to these target sequences were synthesized, and evaluated by transient transfection of CHO-synuclein cells followed by quantitative nIR-fluorescent western blot. Two of the siRNAs, corresponding to positions 270 and 526 of the *Snca* transcript caused highly significant knockdown of α-synuclein in multiple experiments, whereas siRNA404 showed little activity under multiple conditions. Each data point shows the mean of four experiments (error bar shows standard error). *p<0.05, **p<0.01, 1-way ANOVA with Dunnet's *post hoc* test comparing indicated group with control mock-transfected cells.

D: Of the identified siRNAs, siRNA526 showed robust, highly reproducible and concentration-dependent knockdown of α-synuclein expression. siRNA526 also contained the maximal number of mismatches to the SNCB and SNCG transcripts.

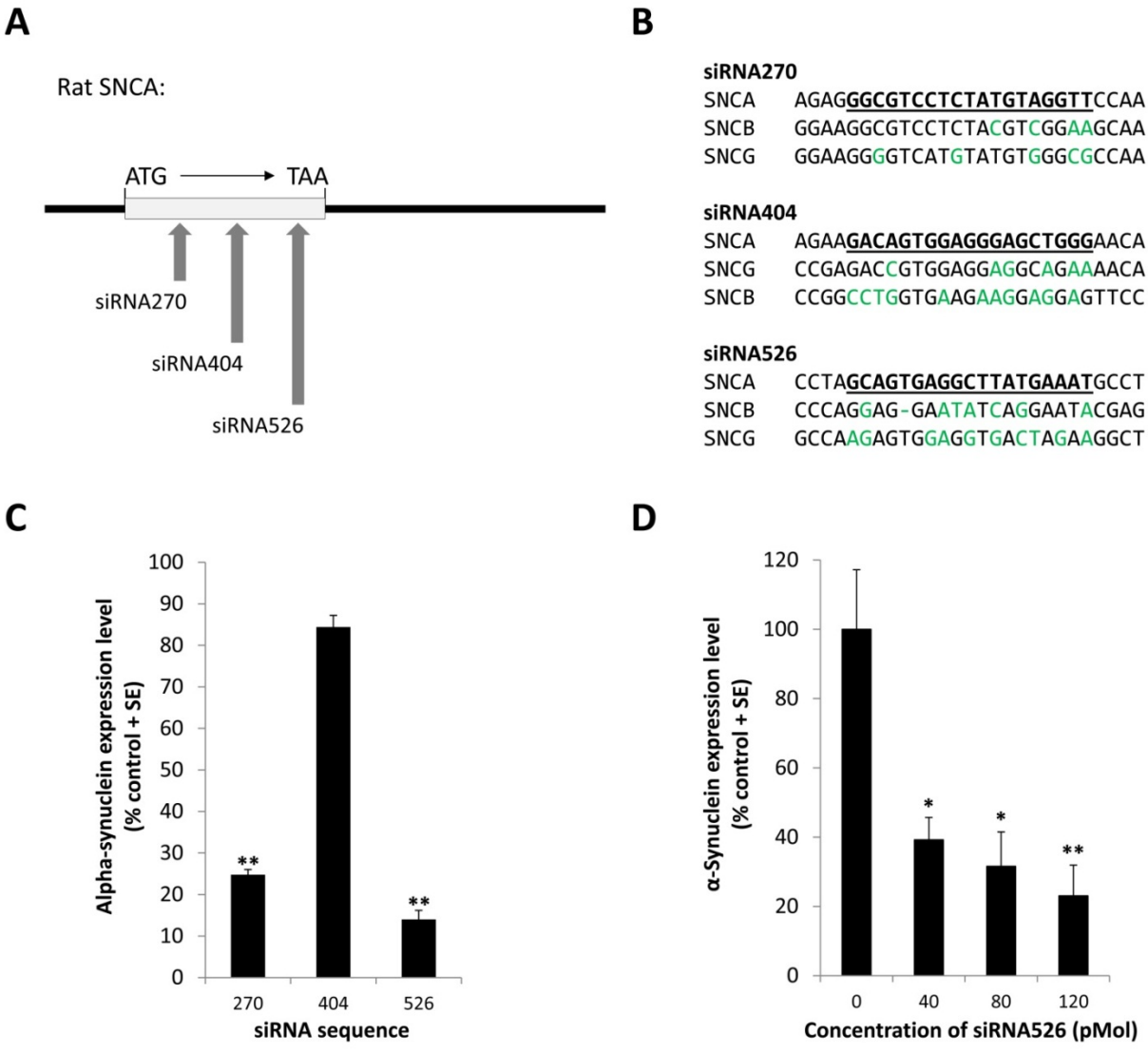

Supplemental Figure 3: Generation of an AAV2 vector expressing shRNA526

A: DNA sequence corresponding to siRNA526 in sense and antisense orientations, separated by a loop sequence (TTCAAGAGA), was cloned into an AAV2 plasmid vector, such that the resulting RNA hairpin was under transcriptional control of the U6 (Pol-III) promoter. The vector was modified from pAAV-D(+)-U6-siRNA-CMV-zsGreen (a kind gift from Dr Bing Wang, Department of Orthopedics, University of Pittsburgh) to express GFP instead of zsGreen from the cytomegalovirus immediate early promoter.

B: CHO-synuclein cells were transiently transfected with the resulting plasmid, and α-synuclein quantified relative to β-actin by quantitative nIR-fluorescent western blot (see Supplemental Figure 1). For comparison, CHO-synuclein cells were transfected with a control vector that was isogenic except that a non-targeting shRNA replaced shRNA526. The graph shows the means of four independent biological replicates (error bars show standard error of mean; *** p<0.001, 2-tailed unpaired t-test, shRNA526 vs non-targeting shRNA).

These data show that shRNA526 caused a progressive reduction in α-synuclein expression levels over the first 48 hours after transfection compared with the control plasmid. The AAV-sh[SNCA] and AAV-sh[control] vectors used for the *in vivo* studies shown in the manuscript were prepared using these plasmids.

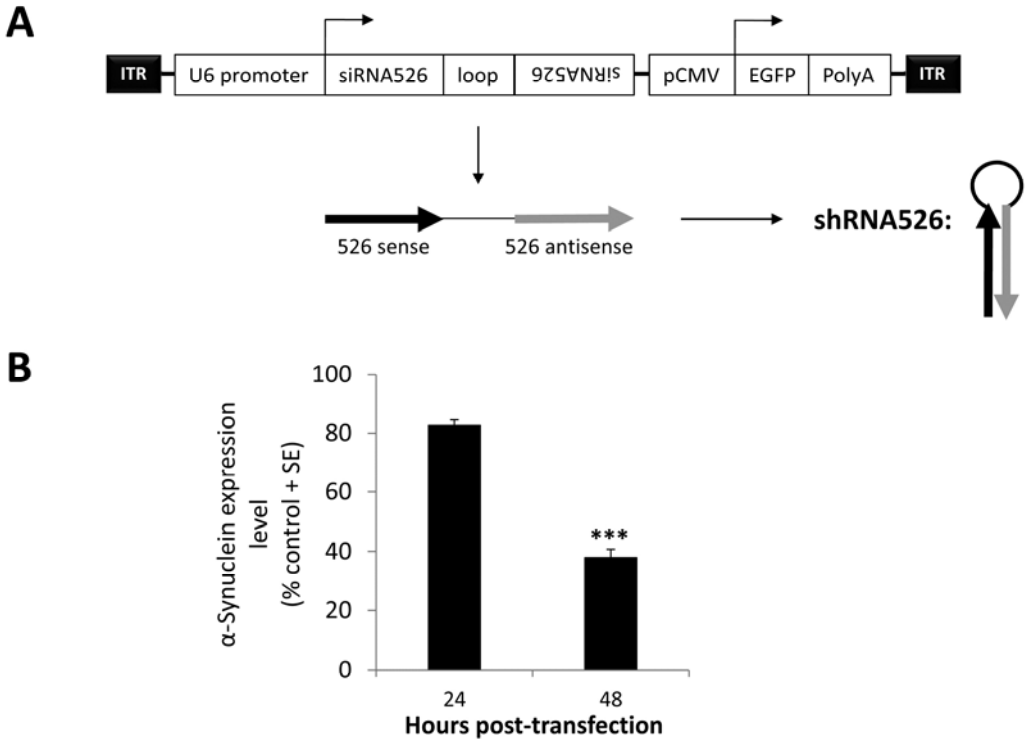

Supplemental Figure 4: Selection of a viral vector for in vivo delivery of shRNA526

An AAV2 vector encoding GFP under transcriptional control of the CMV immediate-early promoter was compared with the same AAV2-GFP genome pseudotyped with AAV serotype 1 or 9 capsid protein for transfection of substantia nigra dopaminergic neurons in the adult rat *in vivo*. Titer-matched vector stocks were infused into the midbrain, dorsal to the substantia nigra. Twenty-one days later, animals were perfused and GFP immunoreactivity evaluated on brain sections from the rostral to the caudal extent of the substantia nigra (coordinates to left of each row) and in the striatum. AAV 2 showed extensive transduction of substantia nigra neurons and expression of GFP in their striatal terminals, even when half of the dose was used (rightmost column) and was consequently selected for further *in vivo* experiments. Scale bar for all images is shown in first panel.

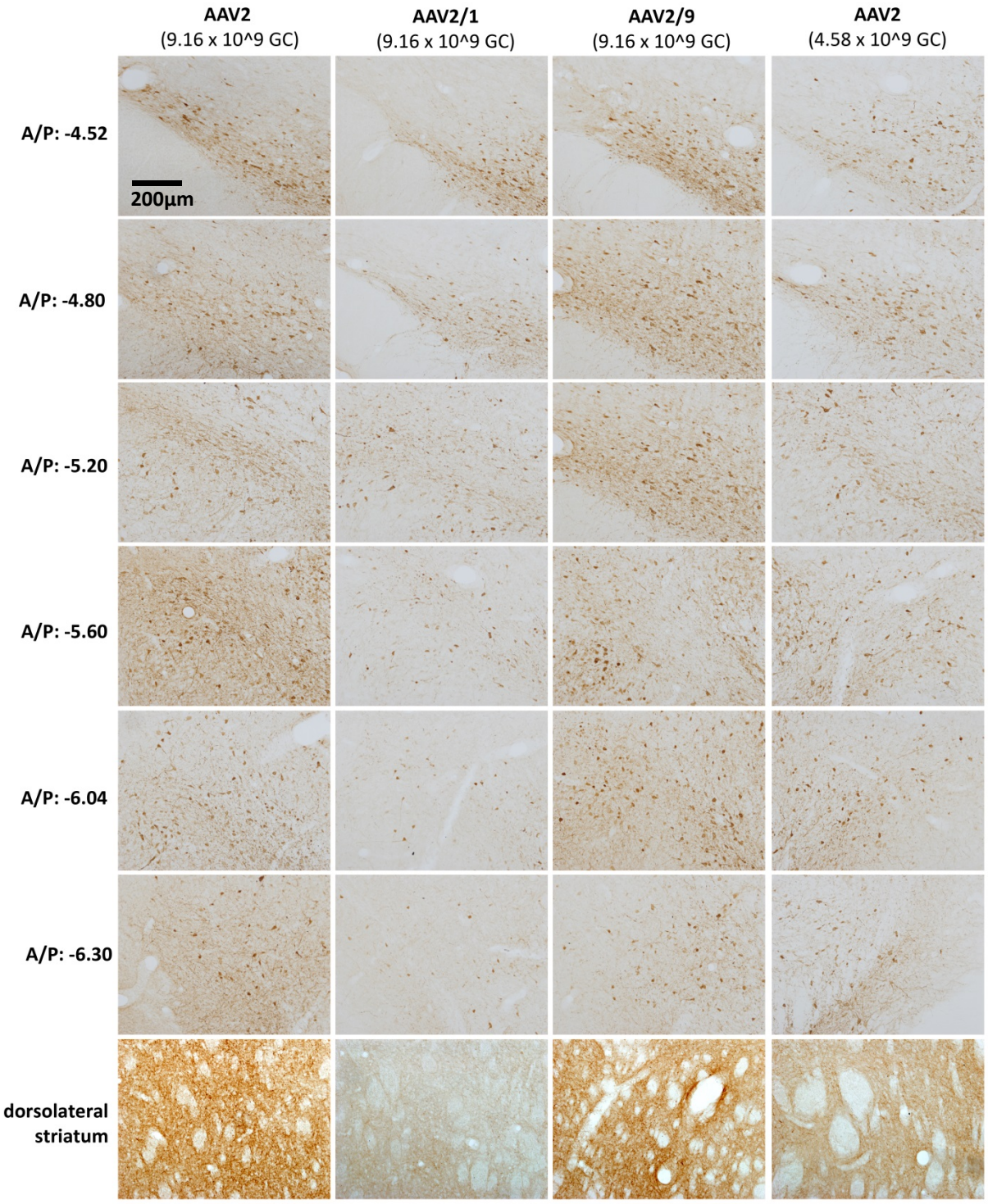

Supplemental Figure 5: Quantification of α-synuclein immunoreactivity in dopaminergic neurons following vector transduction

Animals underwent transduction of the substantia nigra with AAV-sh[SNCA] or AAV-sh[control]. Sections encompassing both sides of the midbrain were immunolabelled for tyrosine hydroxylase and α-synuclein. Confocal imaging was carried out such that the signal was not saturated in either of the channels. Identical acquisition settings were used to image the substantia nigra on each side. Regions of interest corresponding to TH-labeled cell bodies of substantia nigra dopaminergic neurons were drawn by an observer blinded to the α-synuclein channel. α-Synuclein immunoreactive signal was then measured in each region of interest on each side of the brain. For the graphs shown in figure 3C and Supplemental Figures 6 and 8, the α-synuclein signal for each cell on the vector transduced side of the brain was normalized to the mean α-synuclein signal for TH+ neurons on the control side, to allow comparison of how vector transduction affected the distribution of α-synuclein expression (see scatter plots). As shown in the micrographs, the majority of α-synuclein expressed in the substantia nigra is present within nerve terminals, most of which are derived from projections that originate outside the substantial nigra. Immunoreactivity to α-synuclein within the cell bodies of TH positive neurons comprises a small fraction of the total signal. A highly significant ≈ 35% reduction in the cytoplasmic signal was found in neurons transduced with AAV-sh[SNCA] compared with those transduced with AAV-sh[control] or not transduced, although it is likely that this technique underestimates the degree of protein knockdown in the terminals. Similar methodology was employed for figure 5B, C and Supplemental Figure 10 to measure TH expression in nigral dopaminergic neurons.

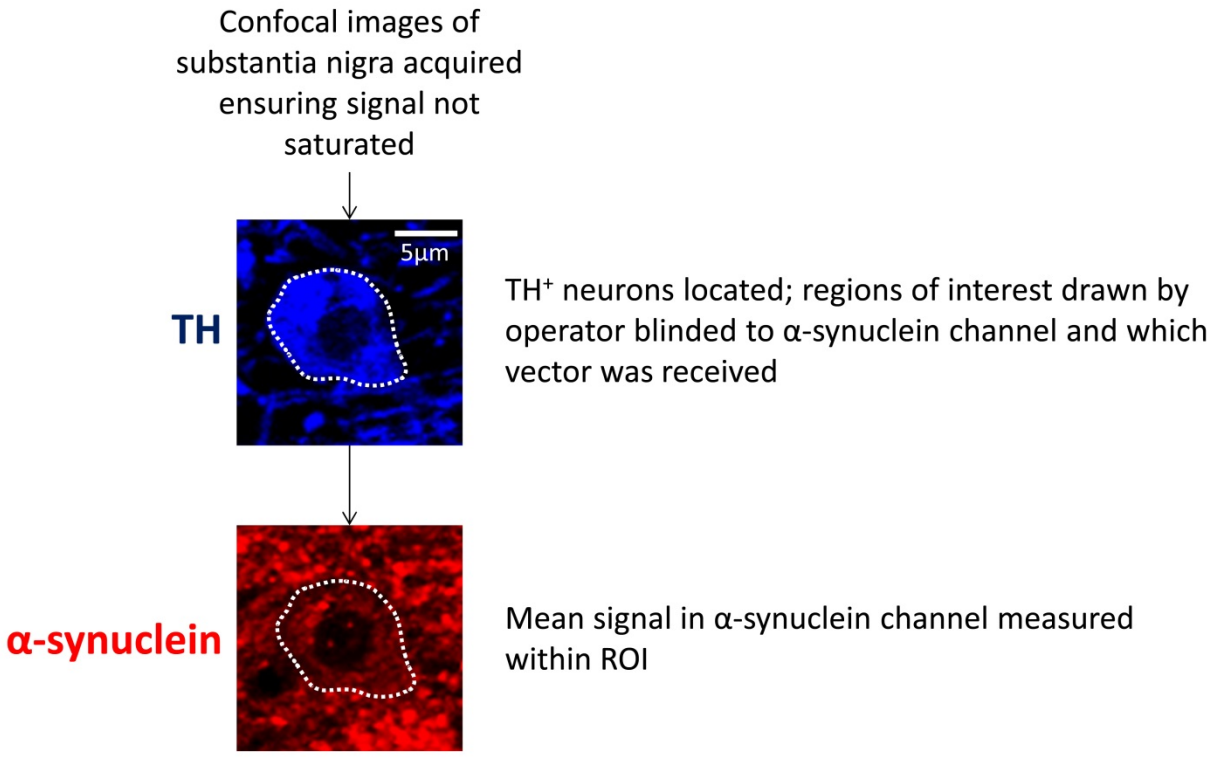

Supplemental Figure 6: Direct comparison of the effects of AAV-sh[SNCA] and AAV-sh[control] on α-synuclein expression in vivo

The data in figures 3C and 3D of the manuscript show that AAV-sh[SNCA] caused a significant ≈35% reduction in α-synuclein expression in substantia nigra dopaminergic neurons *in vivo* compared with non-transduced neurons, using a unilateral transduction experimental design (cohort 2). Using the same experimental design, AAV-sh[control] did not cause a reduction in α-synuclein expression.

The data below show that AAV-sh[SNCA] caused a significant reduction in α-synuclein expression in substantia nigra dopaminergic neurons *in vivo* compared directly with AAV-sh[control], using a bilateral transduction design (cohort 1) in which animals received AAV-sh[SNCA] and AAV-sh[control] on opposite sides of the brain.

A: Cytoplasmic α-synuclein immunoreactivity was quantified in 60 – 100 nigral dopaminergic neurons on each side of each section by confocal imaging. The small markers show α-synuclein immunofluorescence signal for each cell on the vector-transduced side expressed as % of the mean value for dopaminergic neurons on the non-transduced side of the same section. The large markers show mean ± standard error for each animal. The distributions of α-synuclein expression in cells on each side of multiple sections were compared using a 2-tailed unpaired t-test.

B: Mean dopaminergic neuron α-synuclein immunofluorescence is shown for each side of the brain in each animal. Lines join the means for the two sides of each brain. Large markers show mean ± standard error for all three animals. Sides of each animal were compared using a 2-tailed paired t-test.

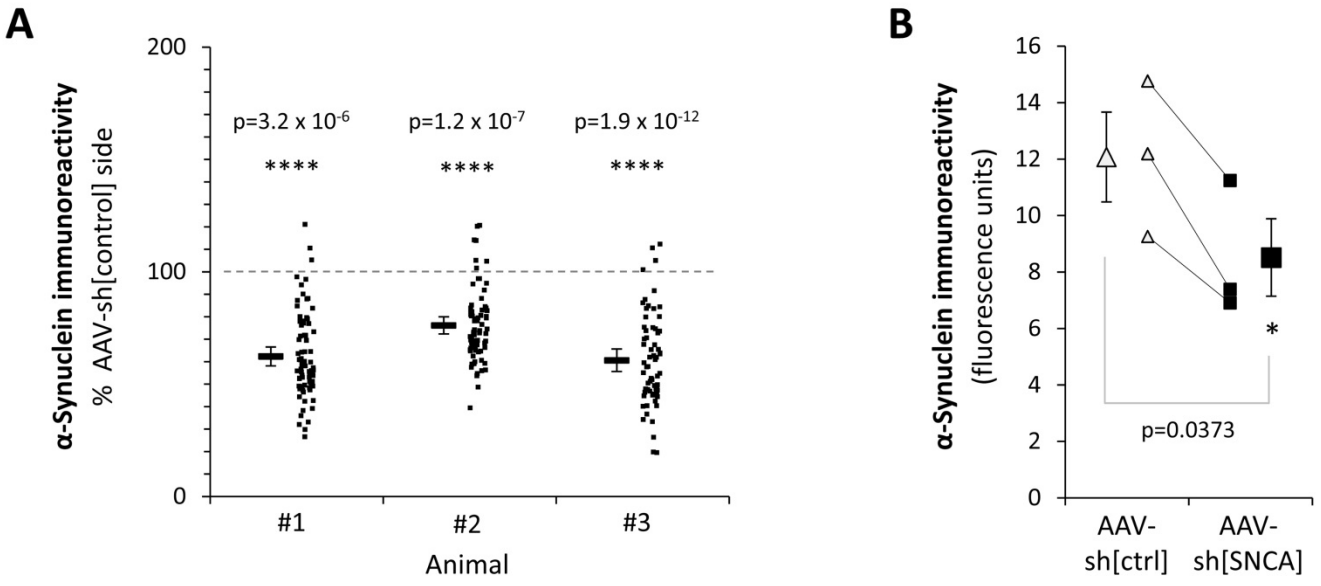

Supplemental Figure 7: Measurement of the integrity of the nigrostriatal projection by quantification of striatal tyrosine hydroxylase immunoreactivity using near infrared quantitative immunofluorescence

Sections encompassing the striatum on both sides were immunolabelled using a primary antibody to TH and a secondary antibody conjugated to a near-infrared fluorophore. The resulting infrared fluorescence signal was quantified using a LICOR scanner with a wide linear range.

A, B: Regions of interest, incorporating the whole striatum (A) or the dorsolateral striatum (B) were drawn by an observer blinded to the treatment the animals received. The mean fluorescence signal within the region of interest was quantified on both sides of the brain and paired statistical test used to determine whether there were significant differences between each side within each animal. The large arrow shows the site of the cortical punch mark used to denote the side that received vector. These pictures are from a rat that did not receive rotenone.

C: The area of each region of interest was also measured. For each experiment, we confirmed that there were no statistically significant differences in the area measured for analysis between the two sides of the brain.

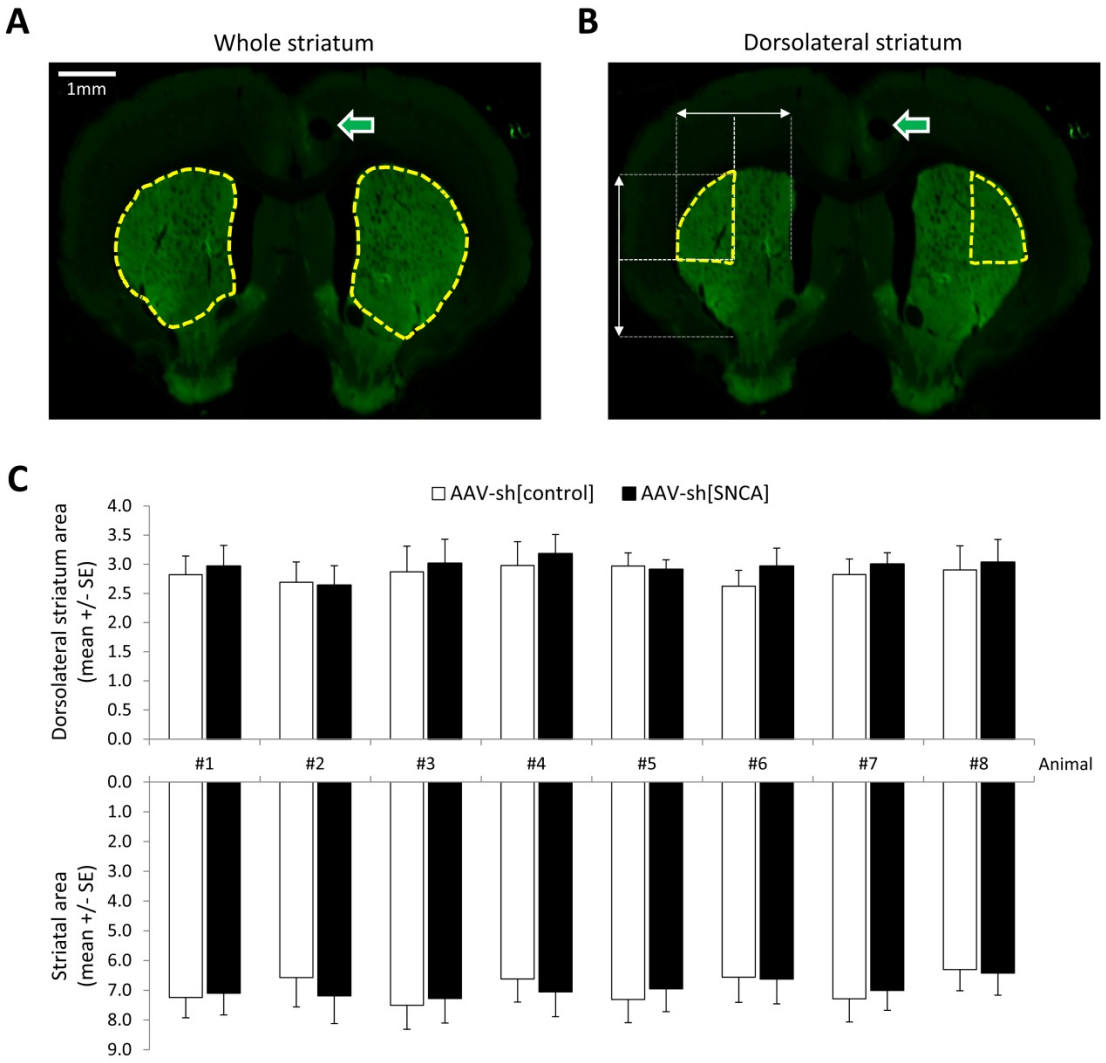

Supplemental Figure 8: AAV-sh[SNCA] prevents accumulation of α-synuclein following rotenone exposure

Cytoplasmic α-synuclein immunoreactivity was quantified in 60 – 100 nigral dopaminergic neurons on each side (non-transduced, white triangles; AAV-sh[control] transduced, grey circles; AAV-sh[SNCA]-transduced, black squares) of midbrain sections from rats in cohort 4 by confocal microscopy. These rats had received rotenone until they reached the study endpoint of >20% reduction in weight or severe global hypokinesia.

A: α-synuclein immunofluorescence signal was quantified on the vector-transduced side and expressed as % of the mean value for dopaminergic neurons on the non-transduced side of the same section. The small markers show each cell and the large markers show mean ± standard error for each animal.

B, C: Mean α-synuclein immunofluorescence signal within dopaminergic neurons is shown for each side of the brain in each animal ('+', vector side; '-', non-transduced control side; lines join the means for the two sides of each brain). (B) AAV-sh[control] transduced brains, (C) AAV-sh[SNCA] transduced brains. Large markers show mean ± standard error for all five animals in each group.

*p<0.05, **p< 0.01, ***p< 0.001, 2-tailed paired t-test, vector transduced side versus control side.

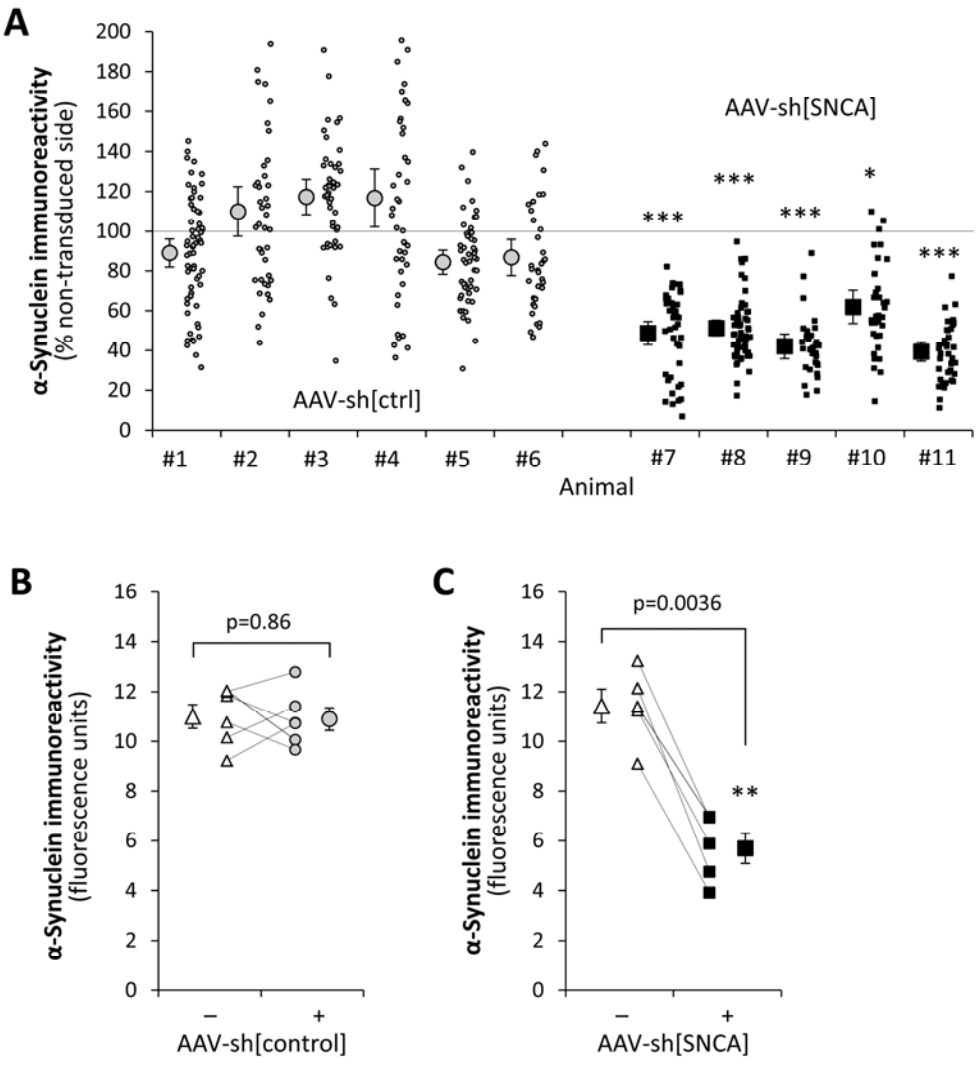

Supplemental Figure 9: Unilateral AAV-sh[SNCA] transduction is neuroprotective compared with unilateral AAV-sh[control] transduction

The data in figures 7, 8 and 9 of the manuscript show that AAV-sh[SNCA] prevents loss of dopaminergic neurons, their striatal terminals and dendrites in the rotenone model of PD. Statistically significant differences were found when AAV-sh[SNCA] was compared with either AAV-[control] (cohort 5) or with no vector (cohort 4). In contrast, measured endpoints did not differ significantly between AAV-sh[control] and no vector (cohort 4).

In order to formally exclude the unlikely possibility that the differences between AAV-sh[SNCA] and AAV-sh[control] observed in the bilateral transduction experiments are attributable to an artifact of the experimental design, we compared the neuroprotective effects of the two vectors in animals that received only unilateral transduction. The graphs show the same data shown in figures 7E, 7F, 8C, 8D, 9C, 9D (cohort 4; unilateral transduction). For each animal, the mean measurement for the vector-transduced side was normalized to the non-transduced side of the same animal, to allow comparison between different animals. The graphs show (A) mean dorsolateral striatal TH immunoreactive signal, (B) total number of dopaminergic neurons by unbiased stereology and (C) mean total neurite length of surviving dopaminergic neurons. Each data point represents a single animal. Key: white triangles, no-vector control animals; white circles, AAV-sh[control]-transduced animals; grey squares, AAV-sh[SNCA]-transduced animals. The dotted line shows a ratio of 1 indicating the measured parameters were equal between the two sides of the brain.

All of the observed differences between AAV-sh[SNCA] and AAV-sh[control] were statistically significant (A: *p<0.05, 1-way ANOVA with Tukey's post-hoc test; B, C: **p<0.01 unpaired 2-tailed t-test). This secondary analysis supports the conclusion that AAV-sh[SNCA] is neuroprotective compared with AAV-sh[control] in the rotenone model. Since the vectors only differ in their shRNA sequence, and there was no difference between no vector and AAV-sh[control], these data confirm that the observed neuroprotective effect of AAV-sh[SNCA] in cohorts 4 and 5 is caused by α-synuclein knockdown.

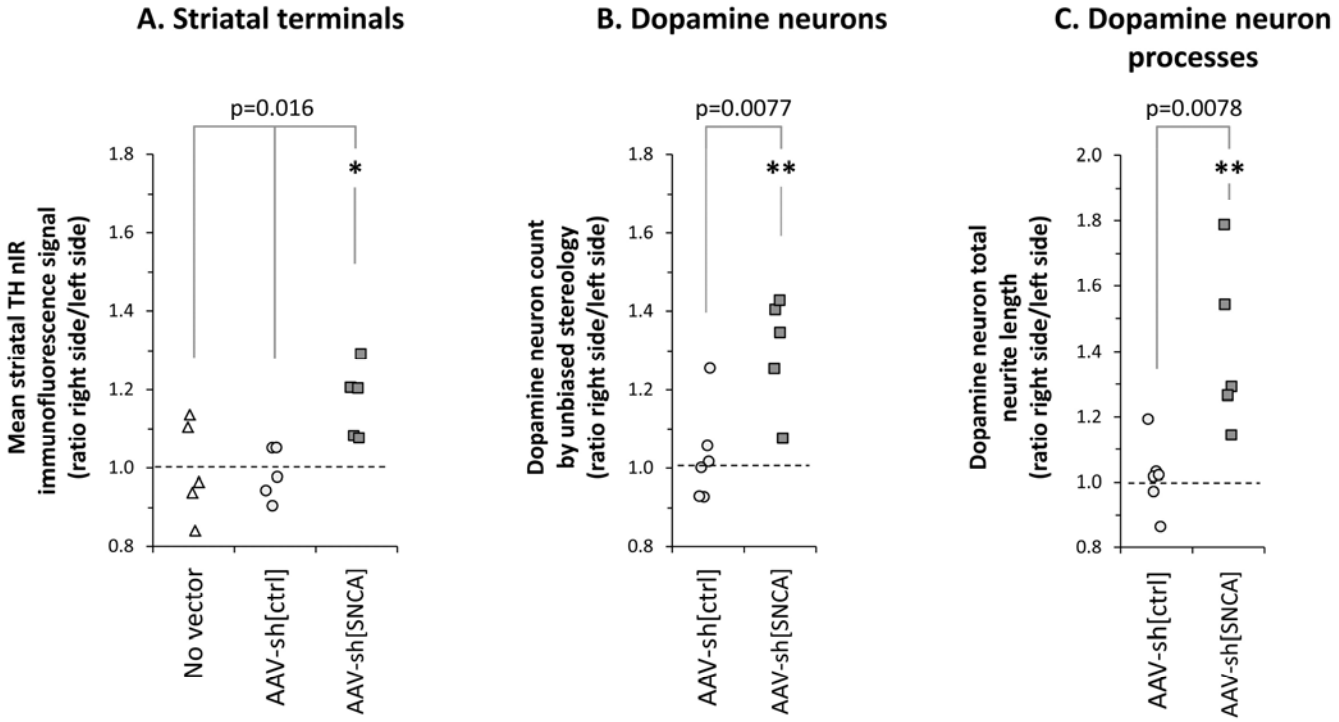

Supplemental Figure 10: AAV-sh[SNCA] does not alter TH expression in dopaminergic neurons after rotenone exposure

To test whether α-synuclein knockdown prevented down-regulation of TH, we measured TH expression in dopaminergic neurons remaining after rotenone exposure. TH immunoreactivity was measured in non-transduced (white triangles), AAV-sh[control] transduced (grey circles) or AAV-sh[SNCA]-transduced (black squares) cells in sections from animal cohort 4. The dotted lines show a value of 100% indicating that TH expression was equal on the transduced and non-transduced sides of the brain.

A: Cytoplasmic TH immunoreactivity was quantified in 60 – 100 nigral dopaminergic neurons on each side of each section by confocal imaging. The small markers show TH immunofluorescence signal for each cell on the vector-transduced side expressed as % of the mean value for dopaminergic neurons on the non-transduced side of the same section. The large markers show mean ± standard error for each animal.

B: Mean dopaminergic neuron TH immunofluorescence is shown for each side of the brain in each animal ('+', vector side; '-' non-transduced side; lines join the means for the two sides of each brain). The left graph shows measurements from animals that were transduced with AAV-sh[control] and the right AAV-sh[SNCA]. Large markers show mean ± standard error for all five animals in each group. Sides were compared using a 2-tailed paired t-test.

C: For each animal, the mean measurement for the vector-transduced side was normalized to the non-transduced side of the same animal, to allow comparison between different animals. Each data point represents a single animal. Key: grey circles, AAV-sh[control] transduced animals; black squares, AAV-sh[SNCA]-transduced animals. Groups were compared using a 2-tailed unpaired t-test.

These data show no evidence that α-synuclein knockdown increased TH expression level in dopaminergic neurons in the rotenone model of Parkinson's disease.

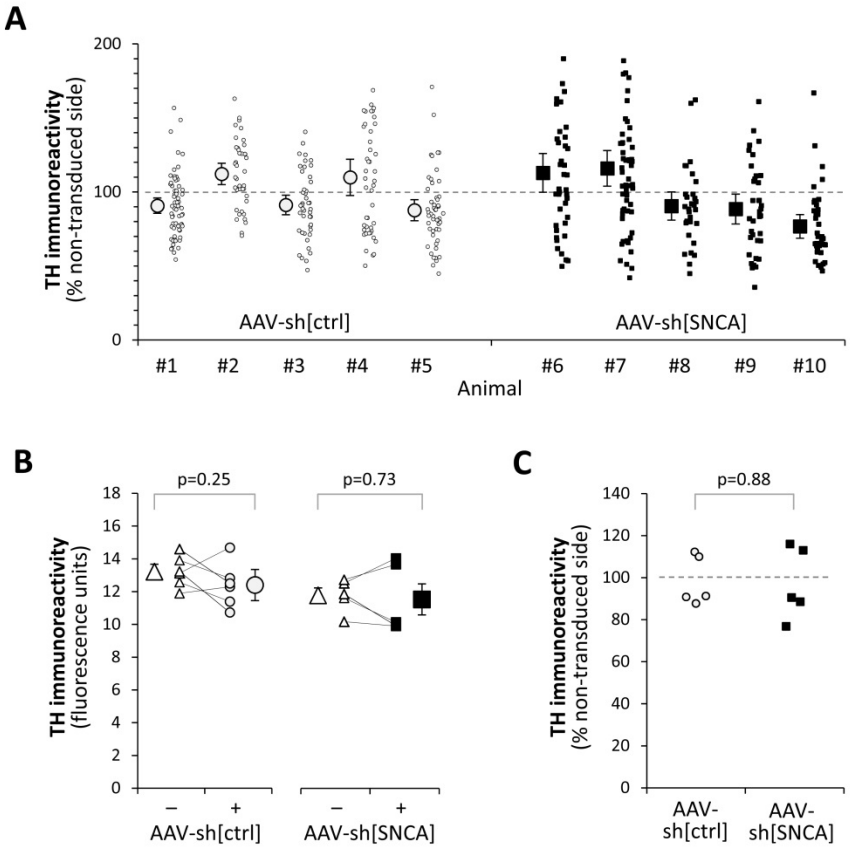

Supplemental Figure 11: α-Synuclein knockdown protects substantia nigra dopamine neurite segments and neurite branches in the rotenone model of Parkinson's disease

Automated image analysis was employed to determine the number of TH-immunoreactive neurite segments (A – C) and the number of neurite branch points (D – F) per surviving TH^+ neuron in the substantia nigra of samples from cohorts 4 (B, C, E, F) and 5 (A, D). The mean values for the two sides of each brain (derived from 5 sections each containing 50 ± 7 dopaminergic neurons), are shown as small markers connected by lines; the large markers show the group mean ± SE. Key: white triangles, non-transduced dopaminergic neurons; grey circles, AAV-sh[control] transduced neurons; black squares, AAV-sh[SNCA]-transduced neurons. p<0.001***, 0.0001****, 2-tailed paired t-test.